# Optical and magnetic properties of the halogen-bridged metal complexes modified by hydrogen bondings: $\{M(1R,2R\text{-cyclohexanediamine})_2Br\}Br_2$ ($M$ = Pt, Pd, and Ni)

H. Okamoto, K. Toriumi, and T. Mitani
*Institute for Molecular Science, Myodaiji, Okazaki 444, Japan*

M. Yamashita
*Department of Chemistry, College of General Education, Nagoya University, Chikusa-ku, Nagoya 464, Japan*
(Received 30 April 1990)

Polarized reflection and ESR measurements have been carried out on single crystals of newly synthesized halogen-bridged one-dimensional (1D) metal complexes $\{M(chxn)_2Br\}Br_2$ ($M$ = Pt, Pd, Ni; chxn = 1$R$,2$R$-cyclohexanediamine), which have tight hydrogen bonds between ligands (chxn) and counter anions ($Br^-$) and construct a two-dimensional (2D) hydrogen-bond network. Both the polarized reflection spectra and the temperature-dependent ESR signals indicate that the electronic state of $M$ = Ni is essentially different from that of $M$ = Pt (or Pd). From the analysis of these results, it can be concluded that the complex for $M$ = Ni is in a monovalent state, where a Mott insulator is formed in a (—$Ni^{3+}$—$Br^-$—) regular chain, in contrast to the mixed-valent state (—$M^{2+}$—$Br^-$—$M^{4+}$—$Br^-$—) for $M$ = Pt and Pd. Thermally excited paramagnetic spins observed for the Pd complex can be explained by the soliton-kink model under the influence of the 2D hydrogen-bond network.

## I. INTRODUCTION

In recent years, one-dimensional (1D) halogen-bridged transition-metal complexes have been extensively studied to clarify the nature of the mixed-valent electronic states as a prototype of the half-filled Peierls-Hubbard system.[1-6] These complexes are represented as $[M^{2+}A_2][M^{4+}X_2A_2]Y_4$ (or simply $\{MA_2X\}Y_2$), where $M$ stands for a transition metal (Pt, Pd, or Ni), $X$ for a halogen ion ($Cl^-$, $Br^-$, or $I^-$), $A$ for a ligand molecule, and $Y$ for a counter anion. The $M^{3+}$-$X^-$ regular chains shown in Fig. 1(a), which have the half-filled band composed of $d_{z^2}$ orbitals of metals, are usually unstable due to the strong electron-lattice interaction.[7-9] It leads to a deviation of the halogen ion from the middle point between the adjacent metal ions as shown in Fig. 1(b).[1,3,5] The resulting state is characterized by the charge-density wave (CDW).[7]

The characteristic feature of the halogen-bridged metal complexes is that their physical properties are strongly dependent on the species of the constituent metal ($M$) and halogen ($X$) ions. Systematic investigations of the $M$ and $X$ dependences of the physical properties in the mixed-valent states have been previously reported in detail. However, the physical properties of the monovalent state have never been clarified. In addition, it seems to be a quite interesting problem how the hydrogen-bond networks between ligands and counter anions affect the electronic states of the one-dimensional $M$-$X$ chains.

Recently, it has been reported that the bromobridged $Ni^{3+}$ complex $[\{Ni(chxn)_2Br\}Br_2]$ does not show Peierls distortion and has ($Ni^{3+}$-$X^-$) linear chain structures.[10] Here, chxn means (1$R$,2$R$)-cyclohexanediamine ligand. This complex was found to have a tight hydrogen-bond network between NH groups of ligands (chxn) and counter anions ($Br^-$). Since the complexes with $Y = ClO_4^-$ $[\{Ni(en)_2X\}(ClO_4)_2$, (en) = ethylenediamine] are in the CDW phase,[11,12] there may be a significant contribution of NH-Br hydrogen-bonds to the stabilization of the regular chain structure (-$Ni^{3+}$-$Br^-$-).

In this paper, we report the results of polarized reflection and ESR measurements of $\{M(chxn)_2Br\}Br_2$ ($M$ = Pt, Pd, and Ni) crystals having two-dimensional (2D) tight hydrogen-bond networks. This represents a unique chance to directly investigate the difference in physical properties, e.g., optical and magnetic ones, of the monovalent state [Fig. 1(a)] and the mixed-valent state [Fig. 1(b)] on the Ni and Pt or Pd complexes, respectively. The $Ni^{3+}$ regular chain[10] is expected to be a one-dimensional spin ($S = \frac{1}{2}$) system. On the other hand, the Pt and Pd complexes, which are in the CDW phase as shown in Fig. 1(b), are essentially diamagnetic. Magnetic properties of the Ni and Pd complexes are discussed in detail on the basis of the temperature dependences of the ESR signals. The influence of the hydrogen-bond network on the physical properties of the 1D $M$-$X$ chain will be elucidated.

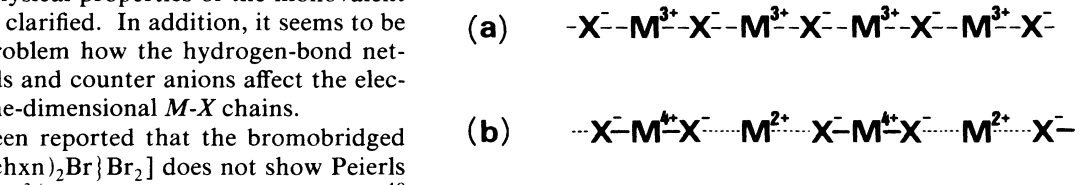


FIG. 1. Linear chain of metals ($M$) and halogens ($X$) in halogen-bridged metal complexes. (a) shows the undistorted state and (b) the CDW state.

 

## II. EXPERIMENT

The complexes $\{M(\text{chxn})_2\text{Br}\}\text{Br}_2$ for $M=$Pt and Pd were synthesized in the same way as reported in Refs. 13 and 14, respectively. The procedure of the sample preparation for $M=$Ni was reported elsewhere in detail.[10] Our complex $[\{\text{Ni(chxn)}_2\text{Br}\}\text{Br}_2]$ is clearly distinguished from the related compound $[\{\text{Ni(chxn)}_2\text{Br}\}\text{Br}_{1.77}]$ which has a different stoichiometry.[15]

In the measurements of polarized reflection spectra, a halogen-tungsten incandescent lamp was used. Light from the lamp was focused by a concave mirror on the entrance slit of a 25-cm grating monochromator (JASCO CT-25). The monochromatic light from the exit slit was passed through a polarizer and was focused by a concave mirror on the specific surface of a single-crystal sample. Reflected light from the sample was focused by a concave mirror on a sensitive position of the detector. As a detector, a PbS cell or a photomultiplier tube was used, depending on the wavelength region.

The ESR measurements were made on single crystals with a standard Varian $X$-band spectrometer (E-112). The temperature of the sample was controlled by an Air-Product (LTD-3-110E) or an Oxford (ESR-9) cryogenic system. The microwave-power dependence of the absorption intensity was checked at several temperatures in order to avoid saturation effects.

## III. EXPERIMENTAL RESULTS AND DISCUSSIONS

### A. Crystal structures

Figure 2 shows the crystal structure of the $Pd^{2+}$-Br-$Pd^{4+}$ complex viewed along the **a** axis.[16] The

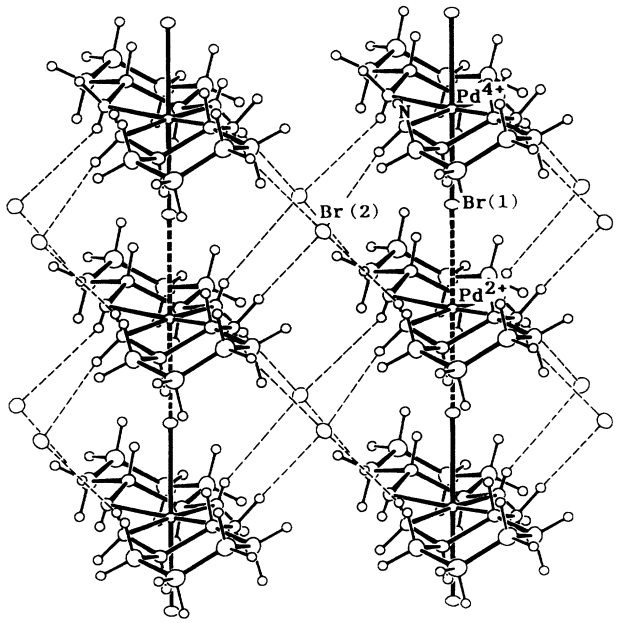


FIG. 2. Crystalline structure of $[\text{Pd(chxn)}_2\text{Br}]\text{Br}_2$ viewed along the **a** axis. Br(1) and Br(2) show the bridging and the counter Br ions, respectively. The dashed lines correspond to the hydrogen bonds.

$Pd^{2+}(\text{chxn})_2$ and $Pd^{4+}(\text{chxn})_2$ units bridged by the $Br^-$ ions are stacked alternately along the **b** axis (the chain axis). The neighboring $Pd(\text{chxn})_2$ moieties on the same chain are linked by the four $\text{NH}\cdots\text{Br}^-\cdots\text{HN}$ intrachain hydrogen bonds which are drawn by the dashed lines in Fig. 2. The hydrogen-bond network is extended over the chains, constructing a 2D structure parallel to the *bc* plane. The crystal structures of the $Pt^{2+}$-Br-$Pt^{4+}$ and $Ni^{3+}$-Br-$Ni^{3+}$ (Ref. 10) complexes are isomorphic to that of the $Pd^{2+}$-Br-$Pd^{4+}$ complex except for the displacements of bridging halogen ions. Details of the crystal structure of $\{M(\text{chxn})_2X\}X_2$ ($M=$Pt and Pd) and $\{\text{Pt(chxn)}_2\text{Cl}\}(\text{ClO}_4)_2$ are planned to be reported elsewhere.[16]

A characteristic feature of this one-dimensional Peierls-Hubbard system can be well described by the structural parameters of the $M\cdots M$ distance $L$, the displacement of halogen ions from the midpoint $\Delta$, and the deformation parameter defined by $d=2\Delta/L$, which are compared for $\{M(\text{chxn})_2\text{Br}\}\text{Br}_2$ ($M=$Ni, Pd, and Pt) in Table I.[16] A notable relation is found among the values of $L$, $\Delta$, and $d$ for the three complexes. With decreasing the $M\cdots M$ distance $L$, both the halogen displacement $\Delta$ and the deformation parameter $d$ decrease. In order to reveal the role of the hydrogen bonds to the $M$-$X$ chain structures, the values of these parameters for $\{\text{Pt(chxn)}_2\text{Cl}\}\text{Cl}_2$ and $\{\text{Pt(chxn)}_2\text{Cl}\}(\text{ClO}_4)_2$ are also listed in Table I.[16] By replacing $Y=\text{ClO}_4^-$ with $\text{Cl}^-$, the considerable decrease of the $M\cdots M$ distance $L$ and the halogen distortion $\Delta$ is found and can be attributed to the increase of the intrachain hydrogen-bond strength ($—N—H\cdots Y\cdots H—N—H\cdots Y\cdots H—N—H\cdots Y\cdots$). [For the complexes $\{M(\text{chxn})_2\text{Br}\}(\text{ClO}_4)_2$ ($M=$Pt, Pd), there is no information about the crystal data.] In the case of $\{\text{Pd(chxn)}_2\text{Br}\}\text{Br}_2$ complex, both $\Delta$ and $d$ show the smallest values among the series of halogen-bridged metal complexes in the CDW phase.

Another role of the hydrogen bonds is demonstrated by the significant interchain interaction observed in the x-ray-diffraction experiments. It has been observed for most of the halogen-bridged mixed-valent complexes that the arrangements of $M^{2+}$ and $M^{4+}$ complexes in the crystals, which are corresponding to the directions of bridging halogen displacements, are not three- or two-dimensionally but one-dimensionally ordered, giving the positional disorder of the bridging halogen ions. As shown in Fig. 2, however, x-ray structure analysis for

TABLE I. Crystal data of the various complexes. $L$ is the metal-to-metal distance, $\Delta$ is the off-center displacement of halogen ions, and $d=2\Delta/L$ is the deformation parameter.

| | $L$ (Å) | $\Delta$ (Å) | $d=2\Delta/L$ |
|---|---|---|---|
| $[\text{Pt(chxn)}_2\text{Br}]\text{Br}_2$ | 5.372 | 0.196 | 0.0730 |
| $[\text{Pd(chxn)}_2\text{Br}]\text{Br}_2$ | 5.296 | 0.125 | 0.0472 |
| $[\text{Ni(chxn)}_2\text{Br}]\text{Br}_2$ | 5.160 | 0 | 0 |
| $[\text{Pt(chxn)}_2\text{Cl}]\text{Cl}_2$ | 5.158 | 0.255 | 0.0989 |
| $[\text{Pt(chxn)}_2\text{Cl}]\text{ClO}_4)_2$ | 5.730 | 0.551 | 0.1923 |

$\{M(\text{chxn})_2\text{Br}\}\text{Br}_2$ complexes ($M$=Pt and Pd) revealed that the directions of the halogen displacements are two-dimensionally ordered in the $bc$ plane. (The CDW state in a chain has two different phases, $\phi$ and $\phi+\pi$, with respect to the displacement of the halogen ions; the CDW on each chain is arranged in phase in the $bc$ plane and forms a 2D ordered structure.) Such 2D ordering of the halogen displacements is attributable to the 2D tight hydrogen-bond network. In the complexes with $Y=\text{ClO}_4^-$ [$\{MA_2X\}(\text{ClO}_4)_2$; $M$=Pt, Pd: $A$=chxn, ethylenediamine (en): $X$=Cl, Br, I], the ordering of the CDW's has not been observed.[16] This might be due to the weak hydrogen-bond network between chains through $\text{ClO}_4^-$ ions.

### B. Optical properties

The polarized reflection spectra of $\{M(\text{chxn})_2\text{Br}\}\text{Br}_2$ crystals ($M$=Pt, Pd, and Ni) are presented in Fig. 3. A strong dispersion is observed for the spectra with an electric vector parallel to the 1D chain ($\mathbf{E}\|\mathbf{b}$). No prominent structure is observed for the $\mathbf{E}\perp\mathbf{b}$ spectra. The imaginary part of the dielectric constants $\epsilon_2$, which are obtained from the reflection spectra for $\mathbf{E}\|\mathbf{b}$ by using the Kramers-Kronig transformation, are shown in Fig. 4. The peak energies of the absorption bands are 1.40, 0.75, and 1.28 eV for the Pt, Pd, and Ni complexes, respectively.

The absorption bands in the spectra of the Pt and Pd complexes are attributable to the charge-transfer (CT) excitations from the fully occupied $d_{z^2}$ orbital of the $M^{2+}$ site to the unoccupied $d_{z^2}$ orbital of the nearest-neighbor

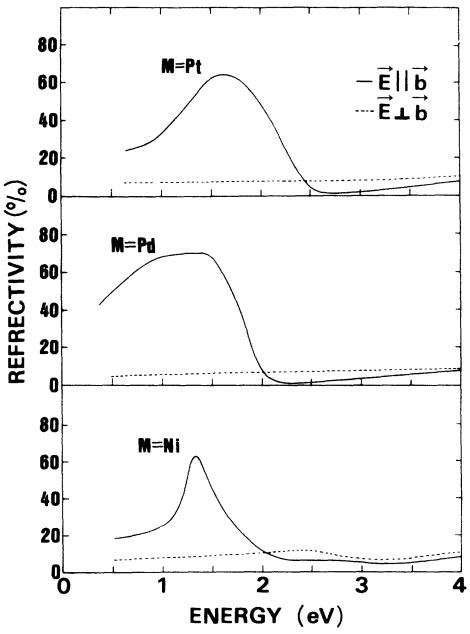


FIG. 3. The polarized reflectivity spectra of $[M(\text{chxn})_2\text{Br}]\text{Br}_2$ ($M$=Pt, Pd, and Ni) with the electric field parallel (solid lines) and perpendicular (dashed lines) to the **b** axis at room temperature.

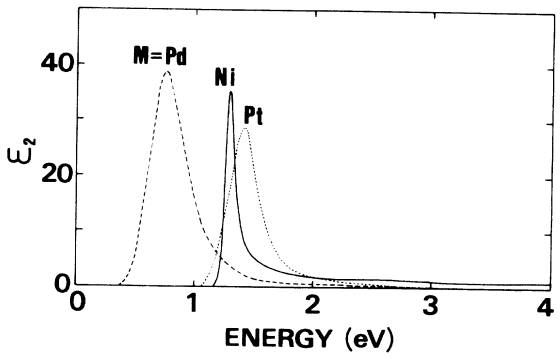


FIG. 4. The imaginary part of dielectric constants transformed from the reflectivity spectra of $[M(\text{chxn})_2\text{Br}]\text{Br}_2$ ($M$=Pt, Pd, and Ni) with the electric field parallel to the **b** axis.

$M^{4+}$ site.[5] The $\epsilon_2$ spectra show a broad and slightly asymmetric Lorentzian shape. This feature is common to the observed spectra of the mixed-valent complexes.[5,6] According to the extended Peierls-Hubbard model, the energy position of the CT excitation $E_{\text{CT}}$ can be given by the parameters $S$, $T$, $U$, and $V$.[7,8] Here, $S$ is the energy of the electron-lattice interaction, $T$ is the transfer energy, and $U$ and $V$ are the on-site and nearest-neighbor Coulomb repulsion energies. In the case that $S$ is much larger than $T$, the lattice relaxation energy $E_s$ by halogen distortions is almost equal to $2S$. If the transfer energy is neglected, $E_{\text{CT}}$ is described as $(2S-U+3V)$.[8,9] When $T$ is introduced in the consideration, $E_{\text{CT}}$ decreases.[8,9] The increase of $U$ due to the decrease of the metal-ion radius could be the main reason for the low-energy shift of the CT excitation by substitution of Pd for Pt. Another reason that could be mentioned is the decrease of the lattice relaxation $E_s$ due to the decrease of halogen distortions. As mentioned above, the distortion parameter $d$ of the $\{\text{Pd}(\text{chxn})_2\text{Br}\}\text{Br}_2$ crystal is the smallest among the mixed-valent complexes, so that the gap energy $E_{\text{CT}}$ shows the smallest value.

The oscillator strengths ($f$) of the CT bands were obtained by integrating the $\epsilon_2$ spectra in the energy region 0.3–4 eV. The $f$ values for the Pt and Pd complexes were determined to be 6.8 and 5.9 for the elementary units ($M$-$X$-$M$-$X$), respectively. As discussed in previous papers,[5,6] the large oscillator strengths can be explained by the intensity transfer from the "$X$-$M$" core CT transition to the "$M$-$M$" CT transition. The former is the CT transition from the filled $p_z$ state of an $X^-$ ion to the empty $d_{z^2}$ state of the nearest-neighbor $M^{4+}$ ion ($X^-+M^{4+}\rightarrow X^0+M^{3+}$) and the latter is the intermetallic CT transition ($M^{2+}+M^{4+}\rightarrow M^{3+}+M^{3+}$). Since both of the two $d_{z^2}$ electrons of a metal and four $p_z$ electrons of a bromine are involved in these transitions, the maximum value of $f$ is 6 for ($M$-$X$-$M$-$X$) unit. The $f$ value higher than 6 for the Pd complex is considered not to be substantial, since there is some ambiguity in both experimental and theoretical view points.

As shown in Fig. 4, the spectrum of the Ni complex seems to be essentially different from those of the Pt and

Pd complexes. The absorption band around 1.3 eV in the Ni complex is considerably sharp and remarkably asymmetric with a long tail in the higher-energy region. In the trans-$[Ni(en)_2Br_2]Br$ complex, which is composed of isolated $Br^-$-$Ni^{3+}$-$Br^-$ units,[17] there was no absorption band corresponding to that observed in the Ni complex around 1.3 eV. Considering that the Ni complex has a 1D chain structure ($-Ni^{3+}$-$Br^-$-), it is quite natural to assign this band to the CT excitation ($Ni^{3+}+Ni^{3+}\rightarrow Ni^{4+}+Ni^{2+}$). Since this Ni complex has no Peierls distortion, as found from the x-ray study, it can be judged to be a typical 1D Mott-Hubbard system. The optical gap $E_{CT}$ is given by ($U$-$V$) in the case of $T=0$. The observed value of $E_{CT}$ (ca. 1.3 eV) for the Ni complex is mainly attributable to Coulomb repulsion energy $U$ on a Ni site.

The oscillator strength of the CT band in the Ni complex was estimated to be 3.0 for a (Ni-Br) unit [or 6.0 for a (Ni-Br-Ni-Br) unit]. The intensity transfer from the $Br^-$-$Ni^{3+}$ transition to the intermetallic CT transition undoubtedly occurs in this complex, as mentioned for the Pt and Pd complexes. The shape of the CT band for the Ni complex is quite sharp compared with those of the mixed-valent complexes ($M$=Pt and Pd). This suggests that the CT excitation is free of the damping effect due to the lattice relaxation. Furthermore, no luminescence could be observed for the Ni complex. These experimental results suggest that the CT exciton of the Ni complex is not relaxed to the self-trapped exciton state, but it moves freely along the chain being delocalized as an electron-hole pair without the local distortions due to the bridging halogen displacement. The long tail of the absorption spectrum in the higher-energy region suggests a presence of another CT transition above 1.5 eV. When $\epsilon_2$ was integrated in the energy region from 1.5 to 4 eV, the oscillator strength of this transition became 1.9 for a (Ni-Br) unit. From these results, one can assume that the core CT transition ($Br^-$-$Ni^{3+}$ transition) locates in the tail region and is strongly mixed with the intermetallic $Ni^{3+}$-$Ni^{3+}$ CT transition around 1.3 eV.

### C. ESR and spin susceptibility

The electronic ground states of the halogen-bridged metal complexes $[\{M(chxn)_2Br\}Br_2]$ mentioned here are specified into two different states, i.e., the Mott-Hubbard state in the monovalent Ni complex and the CDW state in the mixed-valent Pt and Pd complexes as demonstrated by the optical measurements. Temperature-dependent ESR measurements of these compounds show quite different behaviors for their spin states as follows.

(1) $\{M(chxn)_2Br\}Br_2$; $M$=Ni. In Fig. 5(a), the intensity of the ESR signal, which is obtained by the product of the peak-to-peak amplitude of the absorption derivatives and the square of the peak-to-peak linewidth $\Delta H_{pp}$, is plotted as a function of temperature for the magnetic field parallel (rectangulars) and perpendicular (triangles) to the stacking axis **b**. These ESR signals were observed around $g=2$ with a Lorentzian line shape. The temperature dependences of the linewidths $\Delta H_{pp}$ are plotted in Fig. 5(b). As seen from Fig. 5(a), the ESR intensity is almost isotropic below 150 K. Above 150 K, the isotropy is not unambiguous due to the broadening of the signals. In order to obtain information on the high-temperature susceptibility, the ESR spectra were measured using a large amount of randomly oriented crystalline material. The results are presented in the form of an integrated spin susceptibility $\chi_s$ in Fig. 6. The lower-temperature data are also plotted in Fig. 5(a) as solid circles for a comparison. As seen from Figs. 5(a) and 6, $\chi_s$ is insensitive to temperature down to about 50 K and then rapidly increases at lower temperatures. The latter dependence is

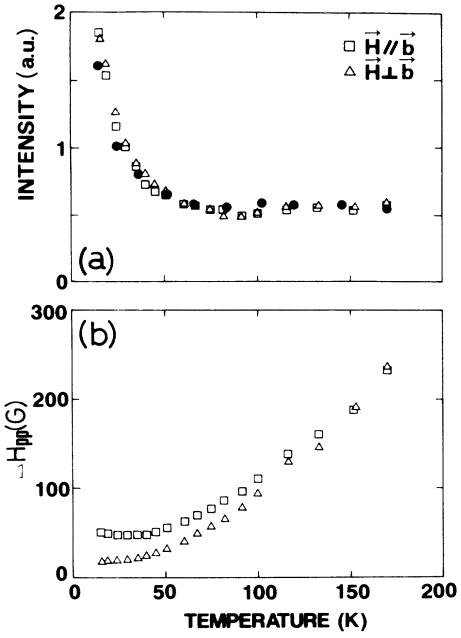


FIG. 5. Temperature dependences of (a) the ESR intensity and (b) the linewidth of $[Ni(chxn)_2Br]Br_2$ for the magnetic field parallel (rectangulars) and perpendicular (triangles) to the **b** axis. The solid circles in (a) are the ESR intensity for randomly oriented single crystals.

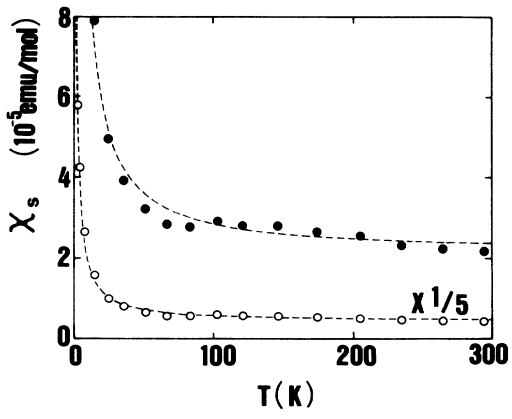


FIG. 6. Temperature dependence of the spin susceptibility of $[Ni(chxn)_2Br]Br_2$. The dashed lines represent the linear combination of the Bonner-Fisher curve and the Curie curve.

closed to the Curie law. Subtracting the Curie-like component from the observed $\chi_s$, the residual component is almost temperature independent. Its absolute value is about $2\times10^{-5}$ emu/mol.

A tentative interpretation of the characteristic magnetic feature observed for the Ni complex, the nearly isotropic intensity and the temperature-independent behavior, can be made by using the 1D Heisenberg ($S=\frac{1}{2}$) model with a large antiferromagnetic exchange interaction ($J$). Calculations of $\chi_s$ were made by applying the Bonner-Fisher formula[18] with an exchange energy $J$ of 3600 K and the Curie spin concentration of 0.22%. The dashed curve in Fig. 6 represents the sum of both terms. The Curie-like component may arise from a residual spin ($=\frac{1}{2}$) in domains or short chains consisting of an odd number of $Ni^{3+}$ ions, which might be produced by the introduction of $Ni^{2+}$ sites in the 1D antiferromagnetic chains.

As mentioned above, $E_{CT}$ is approximately given by ($U$-$V$) under the condition $T=0$. Since $E_{CT}$ is a decreasing function of $T$, ($U$-$V$) should be considerably larger than $E_{CT}$ 1.3 eV. Taking into account the band calculations[19] and the analysis of the simple trimer model,[6] $T$ is around 0.3–0.6 eV for the Pt complexes. The experimental value of $J\sim3600$ K for $\{Ni(chxn)_2Br\}Br_2$ is of the same order of magnitude as the value estimated by the relation $J=4T^2/(U-V)$.[20]

The peak-to-peak linewidth $\Delta H_{pp}$ increases monotonically with increasing temperature as shown in Fig. 5(b). The $g$ factor is anisotropic ($g_{\parallel}=2.021$, $g_{\perp}=2.171$ at 70 K) and almost constant in the measured temperature region. The anisotropy of the $g$ factor indicates that the quenching of the orbital angular momentum is incomplete. In this case, the spin-phonon interaction through the spin-orbit coupling shortens the relaxation time at high temperatures.[21] The monotonical increase of $\Delta H_{pp}$ may be accounted for by this relaxation process.

In our ESR experiments, no spin ordering was detected even at the temperature down to 20 K. (If antiferromagnetic ordering occurs, some changes in the line shape and $g$ values, and the anisotropy of spin susceptibility, should be observed.) The lack of the long-range antiferromagnetically ordered state in spite of the large effective $J$ value may be related to the instability associated with the purely one-dimensional electronic (spin) state.

The measurements of the electrical conductivity along the $b$ axis on the Ni complex showed a semiconducting behavior with a room-temperature conductivity of about 0.5 $s$/cm, which is extremely larger than those of the typical mixed-valence complexes by more than 6 orders.[22,23] The activation energy of about 0.16 eV is remarkably smaller than the optical gap of $E_{CT}=1.28$ eV. The high conductivity and the small activation energy are puzzling, suggesting a presence of some low-energy carriers related to the instability of the 1D Hubbard system. Dynamics of the 1D electronic (spin) system with the extremely large $J$ is an attractive but unknown subject, and more detailed studies from both the experimental and theoretical points of view are required.

(2) $\{M(chxn)_2Br\}Br$; $M$=Pd and Pt. The results of the ESR measurements are clearly different between the two mixed-valent complexes ($M$=Pt and Pd). In the Pt complex, no ESR signal was detected. On the other hand, the ESR signals of the Pd complex due to $S=\frac{1}{2}$ spins showed the characteristic temperature dependence. The difference in the magnetic properties between the two complexes ($M$=Pt and Pd) will be discussed in detail on the basis of the structural parameters described previously in Sec. III A.

The ESR signals of the Pd complex were observed at $g_{\parallel}=2.006$ and $g_{\perp}=2.112$ at room temperature and can be ascribed to the paramagnetic spins of $Pd^{3+}$. The temperature dependence of the integrated intensity of the ESR signals is presented in Fig. 7 as a double logarithmic plot $[\log_{10}(\chi_s)-\log_{10}(T)]$. At low temperatures below 100 K, $\chi_s$ follows the Curie law as shown by the dashed line. This indicates that a constant number of noninteracting $Pd^{3+}$ spins exists in the 1D chain. The concentration of $Pd^{3+}$ spins is about $4\times10^{-3}$ per Pd site, which is 1 order of magnitude lower than the value reported for the powder sample by Toftlund *et al.*[14] Above 100 K, $\chi_s$ deviates from the straight line and increases with increasing temperature. It indicates a thermal excitation of paramagnetic spins. The component of the thermally excited spins $\tilde{\chi}_s$, which can be obtained by subtracting the Curie component from the observed $\chi_s$, was found to follow the activation-type formula $\ln(\tilde{\chi}_s T)\alpha 1/T$ with an activation energy of about 370 K.

The ESR signals show a remarkable narrowing above 100 K. This temperature is almost coincident with the beginning of the thermal excitation of spins; the peak-to-peak linewidth $\Delta H_{pp}$ decreases from 42 G at 140 K to 20 G at 300 K for H⊥b. This behavior can be explained by the motional narrowing effect of the thermally excited spins.

To interpret an origin of the mobile $Pd^{3+}$ paramagnetic spins, the soliton-kink model should be most suitable. The soliton-kink is produced by the phase mismatching of the Peierls distortions. The application of the soliton-

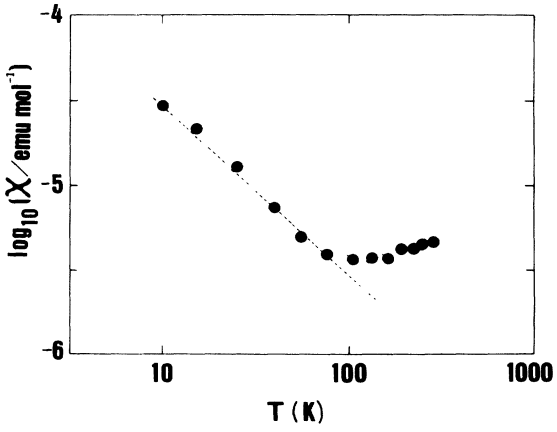


FIG. 7. Temperature dependence of the spin susceptibility of $[Pd(chxn)_2Br]Br_2$. The dashed line represents the component following the Curie law.

kink model to the mixed-valent halogen-bridged metal complexes has been made from the theoretical point of view before.[24,25] The contribution of the effect of the 2D hydrogen-bond network, which will be mentioned below, is considered in our interpretation of the ESR signals based on the soliton-kink model.

From the crystallographic works of these complexes, it has been found that the physical properties of the CDW states are sensitive to the interchain interactions, especially hydrogen bonds. When the amplitude of the CDW state (i.e., the displacement of the halogen ions) is large, the 2D ordering of phases in the CDW states is stiffly locked to the lattice by a cooperation with the interchain hydrogen-bond network. The 2D ordering state of the CDW's means that the CDW's on the respective chains are arranged in phase, as mentioned in Sec. III A. In this case, the soliton-kink is hardly formed in the chain. This is the case of the Pt complex. On the contrary, when the amplitude of the CDW is quite small, the phase ordering will be easily disturbed even at a finite temperature, and then the CDW state becomes one dimensional. Thus, the change of the amplitude of the CDW leads to the change of the dimensionality. In a nearly 1D system, soliton-kinks can be easily formed at high temperatures. As shown in Table I, the distortion parameter $d$ of the Pd complex is the smallest among the mixed-valence complexes in the CDW phase. Accordingly, the thermal excitation of spins in the Pd complex can be well interpreted by the soliton-kinks formed in the quasi-1D chain. Since the ESR signals show the motional narrowing above about 100 K, it is considered that the soliton-kink is not bound but moves freely in the chain. Following the soliton-kink model, the $Pd^{3+}$ spins at low temperatures which follow the Curie law could be attributed to soliton like spins bound by some lattice imperfections.

(3) The other mixed-valent complexes; $\{Pt(en)_2X\}(ClO_4)_2$. As previously reported,[26] the ESR signals of the Pt complexes $[\{Pt(en)_2X_2\}(Y)_2$; $Y=ClO_4^-]$ follow the Curie law in the whole temperature region below the room temperature. The concentration of defects was estimated to be 1–2 per ten thousand Pt sites in common and almost independent of the bridging halogens ($X$=Cl, Br, or I). However, the $Pt^{3+}$ defects in $\{Pt(chxn)_2Br\}Y_2$ ($Y=Br^-$) could not be detected within the sensitivity of our ESR equipment, indicating that the concentration of $Pt^{3+}$ spins is at least 1 order of magnitude lower than that of the $Y=ClO_4^-$ complex. The significant decrease in the number of defects caused by replacing $ClO_4^-$ by $Br^-$ can be ascribed to the increase of the dimensionality of the CDW state, as suggested previously. In the case of $Y=ClO_4^-$, the hydrogen-bond network is considerably weak, so that the solitonlike $Pt^{3+}$ defects are easily introduced in the 1D chains possibly during the crystallization process. These $Pt^{3+}$ defects, however, are naturally localized and bound, because of the large stabilization energy of the halogen displacements.

As discussed above, the introduction of the strong hydrogen bonds causes the two distinctive effects to the formation of soliton kinks. One is the increase of the interchain coupling between the CDW states in neighboring chains. Another is the suppression of amplitude of the CDW. The latter is favorable for reducing the formation energy of the soliton kinks. In the complex having the small amplitude of the CDW (e.g., $M$=Pd, $Y=Br^-$), thermally excited spins of the soliton kinks are observable beyond a signal level of the Curie component. These experimental results suggest a new possibility that the soliton state is well controlled by modifying the strength of hydrogen bondings. Such an attempt, including the high-pressure study, is now under way.

## ACKNOWLEDGMENTS

We are grateful to Professor R. Ikeda, Professor K. Nasu, and Dr. K. Iwano (IMS) for many enlightening discussions. Part of this work was supported by a Grant-in-Aid from the Ministry of Education, Science and Culture, Japan.

[1]H. J. Keller, in *Extended Linear Chain Compounds*, edited by J. S. Miller (Plenum, New York, 1983), Vol. 1, p. 357.
[2]H. Tanino and K. Kobayashi, J. Phys. Soc. Jpn. **52**, 1446 (1983).
[3]R. J. H. Clark, in *Advances in Infrared and Raman Spectroscopy*, edited by R. J. H. Clark and R. E. Hester (Heyden, London, 1984), Vol. 11, p. 95.
[4]H. Tanino, N. Koshizuka, K. Kobayashi, M. Yamashita, and K. Hoh, J. Phys. Soc. Jpn. **54**, 483 (1985).
[5]Y. Wada, T. Mitani, M. Yamashita, and T. Koda, J. Phys. Soc. Jpn. **54**, 3143 (1985).
[6]Y. Wada, T. Mitani, K. Toriumi, and M. Yamashita, J. Phys. Soc. Jpn. **58**, 3013 (1989).
[7]K. Nasu, J. Phys. Soc. Jpn. **52**, 3865 (1983).
[8]K. Nasu, J. Phys. Soc. Jpn. **53**, 302 (1984).
[9]K. Nasu, J. Phys. Soc. Jpn. **53**, 427 (1984).
[10]K. Toriumi, Y. Wada, T. Mitani, S. Bandow, M. Yamashita, and Y. Fujii, J. Am. Chem. Soc. **111**, 2341 (1989).
[11]M. Yamashita, Y. Nonaka, S. Kida, Y. Hamaue, and R. Aoki, Inorg. Chim. Acta **52**, 43 (1981).
[12]G. C. Papavassiliou and D. Layek, Z. Naturforsch. **37b**, 1406 (1982).
[13]K. P. Larsen and H. Toftlund, Acta Chem. Scand. **A31**, 182 (1977).
[14]H. Toftlund, P. W. Jensen, and C. S. Jacobsen, Chem. Phys. Lett. **142**, 286 (1987).
[15]H. Toftlund and O. Simonsen, Inorg. Chem. **23**, 4261 (1984).
[16]K. Toriumi *et al.* (unpublished).
[17]K. Toriumi *et al.* (unpublished).
[18]J. C. Bonner and M. E. Fisher, Phys. Rev. **135**, A640 (1964).
[19]M. Whangbo and M. J. Foshee, Inorg. Chem. **20**, 113 (1981).
[20]M. Takahashi, J. Phys. C **10**, 1289 (1977).
[21]B. N. Figgis, in *Introduction to Ligand Fields*, edited by J. Weiley (Interscience, New York, 1966).

[22]Y. Hamaue, R. Aoki, M. Yamashita, and S. Kida, Inorg. Chim. Acta **54**, 13 (1981).
[23]R. Aoki, Y. Hamaue, S. Kida, M. Yamashita, T. Takemura, and Y. Furuta, and A. Kawamori, Mol. Cryst. Liq. Cryst. **81**, 301 (1982).
[24]S. Ichinose, Solid State Commun. **50**, 137 (1984).
[25]Y. Onodera, J. Phys. Soc. Jpn. **56**, 250 (1987).
[26]A. Kawamori, R. Aoki, and M. Yamashita, J. Phys. C **18**, 5487 (1985).